

Real Time Data Verification of Load and Pressure Testing Using von Mises Yield Criterion for Thick Walled Tubular Products

Donnie Curington

Stress Engineering Services Inc, Measurement and Controls Group, Houston, Texas, USA

Email: donnie.curington@stress.com

Abstract—The oil and gas industry requires standardized testing of tubular products. Testing to the edges of a specified test envelope or yield criterion is performed in order to qualify designs. The most commonly used yield criterion for ductile steel tubular products is the von Mises-Hencky theory which provides a yield criterion based on a triaxial stress state. The yield criterion is used with real time data to model and predict possible impending yield of a test sample and provide notification to a test operator. For a significant portion of the standardized testing, the form of the yield criterion is an ellipse based on a triaxial stress state created by axial, hoop and radial stresses. The criterion is converted to axial loads and pressures and divided into two independent biaxial stress states that are recombined to provide the resultant yield surface or test envelope. The yield equations can be transformed such that a radial stepping technique can be used to produce a calculated yield surface that has the requisite resolution to define the areas of rapid curvature change. The algorithm presented provides sufficient resolution for real time comparison of loads to the yield surface or test envelope to predict possible yielding before potentially damaging expensive test samples.

Index Terms—real time data verification, mechanical testing, thick wall cylinder Lame stresses, triaxial yield criterion, tubular products

I. INTRODUCTION

The oil and gas industry is continuously pushing the limits of tubular product performance with new and improved connection designs. The industry requires testing of these products to API/ISO standards [1], [2]. Testing to the edges of a specified yield criterion or test envelope is performed in order to qualify designs. This testing becomes even more important as the industry pushes the limits in order to reach deeper hydrocarbon reserves [3].

The most commonly used combined stress yield criterion for ductile steel tubular products in the oil and gas industry is the Maximum Distortion Energy Theorem, also referred to as the von Mises-Hencky theory [4]. It provides a ductile yield criterion based on a triaxial stress state. The yield criterion can be used with real time data to model and predict possible impending yield of a test

sample and provide a test operator with a notification. This allows the test operator or load frame itself to perform corrective action to protect the sample.

A significant portion of the standardized testing is done with axial, pressure and thermal loading. In this case the form of the yield criterion can be reduced to an ellipse based on a triaxial stress state resulting from axial loads, internal pressures and external pressures. Using the definition of uniaxial stress along with Lamé equations [5]-[7] for radial and hoop stresses due to internal and external pressures, the von Mises criterion is converted to axial loads and pressures [2], [7]. Once put into this form, the axial load, internal and external pressures cannot be explicitly separated so the equation set is divided into two independent biaxial stress states and two ellipse halves are generated [2]. The internal pressure and axial loads equation set is only valid for the internal pressure half of the calculated ellipse. Likewise, the external pressure and axial load equation set is only valid for the external pressure portion of the calculated ellipse. The two ellipse halves are then recombined to provide the resultant yield surface [2] as shown in Fig. 1.

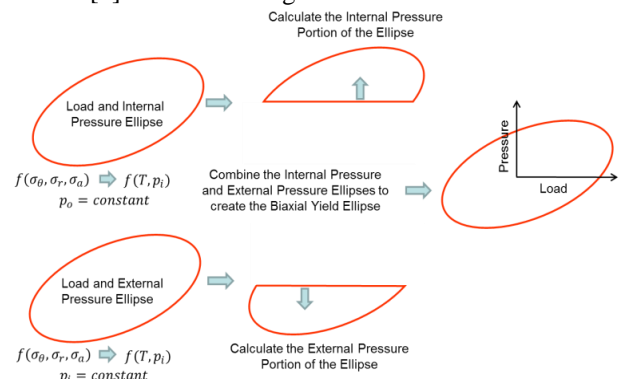


Figure 1. Ellipse generation process.

A. Abbreviations

- a:** inner radius
- b:** outer radius
- p_i:** internal pressure
- p_o:** external pressure
- r:** radial calculation location
- T:** load
- ε:** joint efficiency

Manuscript received January 1, 2018; revised February 11, 2019.

θ : offset angle
 γ : radial sweep angle
 σ_i : principal stress
 S_y : yield strength
 $\alpha_{ij}, \mathbf{A}, \mathbf{B}, \mathbf{C}, \mathbf{D}, \mathbf{E}$: constants
 v_i : vector to calculation points

II. ELLIPSE DEFINITION

Cartesian stepping can be used to generate the yield ellipse but it leads to an unnecessary number of calculations required to adequately represent the areas of rapid curvature needed for real time data checking. This problem is illustrated by the square symbols along the curve in Fig. 2. As the increment of load ΔT_i , or pressure Δp_i , increases toward the outer edge of the ellipse it can be seen that some portion of the curve will be approximated by a straight line. The area of curvature after the last step for incrementing load ΔT_i is highlighted in Fig. 2. It requires a significant reduction in step size to represent the curvature. For the purposes of real time data checking, the resulting yield surface would be too conservative and alarming would occur during normal test operations.

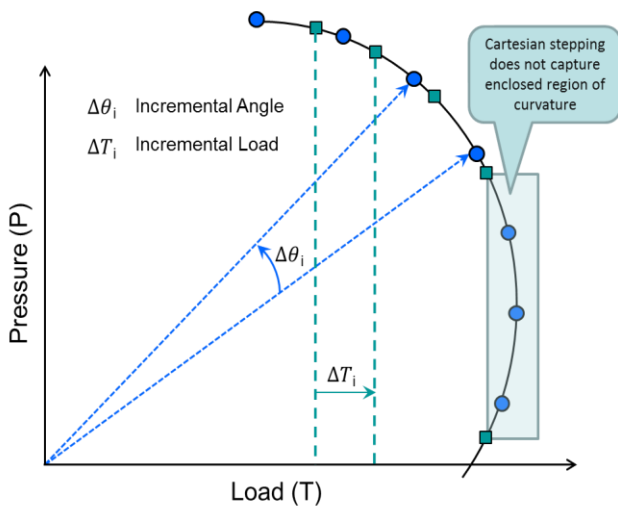


Figure 2. Cartesian and radial calculation stepping.

The ellipse can be transformed so that a radial stepping technique can be used. The algorithm produces the yield surface with the requisite resolution to define the areas of rapid curvature change with substantially less calculation overhead. Fig. 2 illustrates the radial sweep points $\Delta\theta_i$ as circle symbols along the curve. Because of the resolution improvement, interpolations can be made between calculation data points to determine if a load ΔT and pressure Δp window around the real time data is completely inside of the test envelope, it overlaps the envelope or it is completely outside of the test envelope. This allows for real time comparison of loads and pressures to the yield criterion to predict an impending sample yield before potentially damaging expensive test samples.

The general form of the von Mises yield criterion for a triaxial stress state is shown in (1).

$$2S_y^2 = (\sigma_1 - \sigma_2)^2 + (\sigma_2 - \sigma_3)^2 + (\sigma_3 - \sigma_1)^2 \quad (1)$$

For thick wall cylinders, the principal stresses can be shown to be represented by the Lamé hoop and radial stress equations [2], [6] and axial stress. In the absence of bending or torsion, yielding will always occur at the inner radius of the cylinder [2], [8]. Therefore, the calculations can be reduced to one radial location on the sample. The Lamé equations can then be refactored and simplified in terms of constants to be used to generate the von Mises ellipse.

A. Internal Pressure and Axial Loading

The Lamé thick wall cylinder equations for the tangential stress is represented, refactored and simplified in terms of the internal pressure p_i while the external pressure p_o is held constant as shown in (2a-2c).

$$\sigma_\theta|_r = \frac{a^2 p_i - b^2 p_o}{b^2 - a^2} + \frac{a^2 b^2 (p_i - p_o)}{r^2 (b^2 - a^2)} \quad (2a)$$

$$\begin{aligned} \sigma_\theta|_r = & \left[\frac{a^2 r^2 + a^2 b^2}{r^2 (b^2 - a^2)} \right] p_i \\ & + \left[\frac{-p_o b^2 (r^2 + a^2)}{r^2 (b^2 - a^2)} \right] \end{aligned} \quad (2b)$$

$$\sigma_\theta|_r = Ap_i + C \quad (2c)$$

The same process can be done for the radial stress. The Lamé thick wall cylinder equation for the radial stress is represented, refactored and simplified in terms of the internal pressure p_i while the external pressure p_o is held constant as shown in (3a-3c).

$$\sigma_r|_r = \frac{a^2 p_i - b^2 p_o}{b^2 - a^2} - \frac{a^2 b^2 (p_i - p_o)}{r^2 (b^2 - a^2)} \quad (3a)$$

$$\begin{aligned} \sigma_r|_r = & \left[\frac{a^2 r^2 - a^2 b^2}{r^2 (b^2 - a^2)} \right] p_i \\ & + \left[\frac{-p_o b^2 (r^2 - a^2)}{r^2 (b^2 - a^2)} \right] \end{aligned} \quad (3b)$$

$$\sigma_r|_r = Dp_i + E \quad (3c)$$

The axial stress due to tension or compression is independent of pressure and represented and simplified in (4a-4b).

$$\sigma_a = \frac{T}{\varepsilon \pi (b^2 - a^2)} \quad (4a)$$

$$\sigma_a = BT \quad (4b)$$

B. External Pressure and Axial Loading

The Lamé thick wall cylinder equations for the tangential stress at any radial location is represented,

refactored and simplified in terms of the external pressure p_o while the internal pressure p_i is held constant as shown in (5a-5c).

$$\sigma_\theta|_r = \frac{a^2 p_i - b^2 p_o}{b^2 - a^2} + \frac{a^2 b^2 (p_i - p_o)}{r^2 (b^2 - a^2)} \quad (5a)$$

$$\begin{aligned} \sigma_\theta|_r &= \left[\frac{-b^2 r^2 - a^2 b^2}{r^2 (b^2 - a^2)} \right] p_o \\ &\quad + \left[\frac{p_i a^2 (r^2 + b^2)}{r^2 (b^2 - a^2)} \right] \end{aligned} \quad (5b)$$

$$\sigma_\theta|_r = A p_o + C \quad (5c)$$

The same process can be done for the radial stress. The Lamé thick wall cylinder equation for the radial stress is represented, refactored and simplified in terms of the external pressure p_o while the internal pressure p_i is held constant as shown in (6a-6c).

$$\sigma_r|_r = \frac{a^2 p_i - b^2 p_o}{b^2 - a^2} - \frac{a^2 b^2 (p_i - p_o)}{r^2 (b^2 - a^2)} \quad (6a)$$

$$\sigma_r|_r = \left[\frac{a^2 b^2 - r^2 b^2}{r^2 (b^2 - a^2)} \right] p_o + \left[\frac{p_i a^2 (r^2 - b^2)}{r^2 (b^2 - a^2)} \right] \quad (6b)$$

$$\sigma_r|_r = D p_o + E \quad (6c)$$

The axial stresses due to tension or compression are represented and simplified the same as shown in (4a-4b).

C. Ellipse Definition in Conic Form

Substituting the above appropriate internal pressure and axial load equation set (2c,3c,4b) into the von Mises equation (1) using gives (7a-7b)

$$2S_y^2 = (\sigma_\theta - \sigma_a)^2 + (\sigma_a - \sigma_r)^2 + (\sigma_r - \sigma_\theta)^2 \quad (7a)$$

$$\begin{aligned} 2S_y^2 &= (A p_i + C - B T)^2 + (B T - D p_i - E)^2 \\ &\quad + (D p_i + E - A p_i - C)^2 \end{aligned} \quad (7b)$$

In order to change the form into one of a general equation for conic sections [5], (7) can be refactored into the form of (8)

$$\begin{aligned} 0 &= (2B^2) T^2 + 2(-AB - BD) T p_i \\ &\quad + (2A^2 + 2D^2 - 2AD) p_i^2 \\ &\quad + 2(-BC - BE) T \\ &\quad + 2(2AC + 2DE - DC \\ &\quad - AE) p_i + (2(C^2 + E^2 - CE \\ &\quad - S_y^2)) \end{aligned} \quad (8)$$

The yield ellipse is now defined by the general equation for conic sections [9] shown as (9a-9b)

$$\begin{aligned} 0 &= \alpha_{11} T^2 + 2\alpha_{12} T p_i + \alpha_{22} p_i^2 + 2\alpha_{13} T \\ &\quad + 2\alpha_{23} p_i + \alpha_{33} \end{aligned} \quad (9a)$$

where α_{ij} is defined as

$$\alpha_{ij} = \alpha_{ji} \quad (9b)$$

III. ELLIPSE TRANSFORMATION

The ellipse is generated as shown in Fig. 3 by calculating the major axis a , the minor axis b and radially calculating the points based on the desired angular resolution of the sweep angle γ .

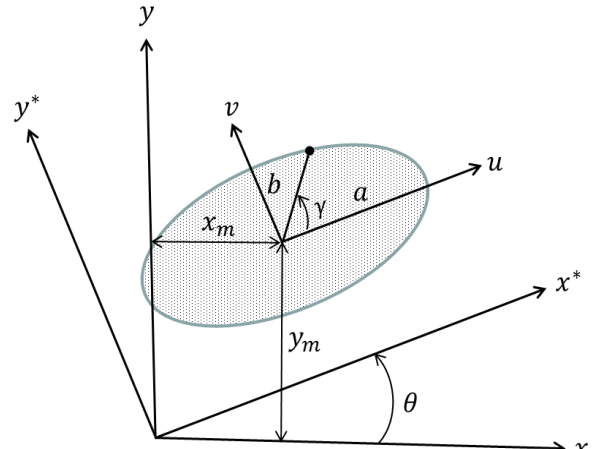


Figure 3. Ellipse u-v to x-y transformation.

Fig. 3 also illustrates the transformation from the local u-v ellipse coordinate system to the global x-y coordinate system. Constants composed of the invariants [9] required for the transformation are defined in equations (10a-10c)

$$I_1 = \alpha_{11} + \alpha_{22} \quad (10a)$$

$$I_2 = \begin{vmatrix} \alpha_{11} & \alpha_{12} \\ \alpha_{21} & \alpha_{22} \end{vmatrix} \quad (10b)$$

$$I_3 = \begin{vmatrix} \alpha_{11} & \alpha_{12} & \alpha_{13} \\ \alpha_{21} & \alpha_{22} & \alpha_{23} \\ \alpha_{31} & \alpha_{32} & \alpha_{33} \end{vmatrix} \quad (10c)$$

The ellipse can then be generated with respect to the u-v axes and appropriately rotated and translated. The equations of the ellipse in terms of the u-v axes is given as (11a-11c)

$$\beta_{11} u^2 + \beta_{22} v^2 + \beta_{33} = 0 \quad (11a)$$

where β_{11} and β_{22} are defined as

$$\beta_{11}, \beta_{22} = \frac{I_1}{2} \pm \sqrt{\left(\frac{I_1}{2}\right)^2 - I_2} \quad (11b)$$

and β_{33} is defined as

$$\beta_{33} = \frac{I_3}{I_2} \quad (11c)$$

Magnitudes of the principal semi-axes and the direction to the principal axis can be calculated using (12a-12c) where the major axis a is defined as

$$a = \sqrt{\frac{-\beta_{33}}{\beta_{11}}} \quad (12a)$$

and the minor axis b is defined as

$$b = \sqrt{\frac{-\beta_{33}}{\beta_{22}}} \quad (12b)$$

and principle axis rotation angle θ is defined as

$$\theta = \frac{1}{2} \tan^{-1} \left(\frac{2\alpha_{12}}{\alpha_{11} - \alpha_{22}} \right) \quad (12c)$$

where θ is limited to

$$\theta \leq \frac{\pi}{2} \quad (12d)$$

The coordinates of the center point of the ellipse are given using (13a-13b) where the x axis offset x_m is defined as

$$x_m = \frac{\alpha_{12}\alpha_{23} - \alpha_{13}\alpha_{22}}{I_2} \quad (13a)$$

And the y axis offset y_m is defined as

$$y_m = \frac{\alpha_{12}\alpha_{13} - \alpha_{11}\alpha_{23}}{I_2} \quad (13b)$$

The parametric equation coordinates to a point in the u-v plane are given using (14a-14b)

$$[u \ v] = [a \cos \gamma \ b \sin \gamma] \quad (14a)$$

where the sweep angle γ varies as

$$0 \leq \gamma \leq 2\pi \quad (14b)$$

The final transformation into the x-y coordinate system is given using (15a-15b)

$$[x^* \ y^*] = [u \ v] \begin{bmatrix} \cos \theta & \sin \theta \\ -\sin \theta & \cos \theta \end{bmatrix} \quad (15a)$$

The final transformed array $[x \ y]$ is defined as

$$[x \ y] = [x_m \ y_m] + [x^* \ y^*] \quad (15b)$$

The process is done to generate an ellipse for the internal pressure Lamé equation set with axial loads and to generate an ellipse for the external pressure Lamé equation set with axial loads. The calculations are only

performed for the pressures corresponding to internal pressure or external pressure with the respective equation set. The two ellipse halves are combined to represent the resultant yield ellipse or test envelope.

IV. REAL TIME DATA VERIFICATION

The radial sweep ellipse generation technique provides a resolution that can be used for interpolation with real time data. With the linear stepping illustrated in Fig. 2, the location of maximum curvature can miss significant portions of the yield envelope for reasonable calculation step sizes ΔT_i . With a radial sweep $\Delta\theta_i$ the calculated ellipse points can be used to interpolate with a better calculation resolution to determine if the real time data checking window is completely inside, overlapping or completely outside the test envelope. In practice, an operating window around the real time data point is verified as shown in Fig. 4.

Software precalculates the yield surface. For each real time load and pressure data point it checks the four corner points of the incremental load ΔT and pressure ΔP window. The alarming criterion is based on a comparison of the magnitude of each given window corner point vector and the magnitude of the collinear vector to the crossing point of the segment created between the two adjacent radial data points, points p_1 and p_2 , as illustrated in Fig. 4 by the diamond symbol. If during testing, the real time data alarming window overlaps the yield surface the test operator is given a warning. If the entire set of real time data alarming window points are outside of the yield surface, the test operator is presented an alarm state. This provides actionable real time information that is difficult to discern from only the load and pressure measurements.

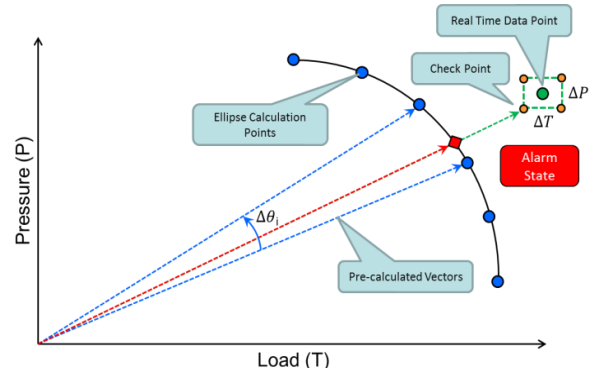


Figure 4. Real time data checking.

V. PRACTICAL IMPLEMENTATION

The practical implementation in software involves precalculating the yield ellipse. The software can precalculate the yield ellipse and retain the coordinates, the vector magnitude and the direction angle to the vector for each yield ellipse calculation point.

A series of quick geometry manipulations can be made based on the real time data checking window in combination with the precalculated angles and magnitudes to the ellipse calculation points. With the

ellipse points calculated at a sufficient resolution, the location of the crossing of the projected vector \vec{v}_c on the ellipse can approximated using the assumption of a straight line segment s_{12} between the two adjacent data points p_1 and p_2 .

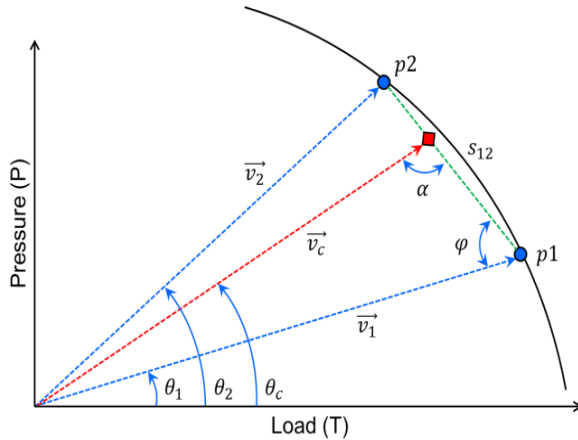


Figure 5. Check vector magnitude.

The magnitude of the segment bounded by the two vectors \vec{v}_1 and \vec{v}_2 is given by (16)

$$s_{12} = \sqrt{v_1^2 + v_2^2 - 2v_1v_2 \cos(\theta_2 - \theta_1)} \quad (16)$$

The interior angle between the segment a and the vector \vec{v}_1 is shown as φ in Fig. 5 and is calculated in (17)

$$\varphi = \cos^{-1} \left(\frac{v_1^2 + a^2 - v_2^2}{2v_1a} \right) \quad (17)$$

The included angle α is defined using the precalculated angle θ_1 to the p_1 vector \vec{v}_1 and to the respective collinear vector defined by the incremental load ΔT and pressure ΔP window data point as shown in Fig. 5.

$$\alpha = \pi - \varphi - (\theta_c - \theta_1) \quad (18)$$

The magnitude of the yield ellipse approximation vector \vec{v}_c can now be calculated as (19)

$$v_c = \frac{v_1 \sin \varphi}{\sin \alpha} \quad (19)$$

Once the magnitude of the yield ellipse approximation vector \vec{v}_c is calculated, it can be compared magnitude of the vector to the associated bounding check point of the real time data checking window.

VI. ALGORITHM SUMMARY

The general procedure to implement the algorithm in software involves a series of precalculated steps and a series of iterative steps:

A. Precalculated Steps (1-5)

1. Obtain the sample parameters; inner radius a , outer radius b and yield strength S_y
2. Calculate the internal pressure portion of the von Mises yield ellipse using the equation sets outlined in the section *II.A Internal Pressure and Axial Loading*
3. Calculate the external pressure portion of the von Mises yield ellipse using the equation sets outlined in the section *II.B External Pressure and Axial Loading*
4. Invert the external pressure calculated points and combine them with the internal pressure calculated points to create a single yield surface.
5. Calculate the magnitude and angle to each ellipse point for the combined curve and retain the values

B. Iterative Steps (6-14)

6. Obtain the real time data point and determine the four bounding checking window points.
7. For each of the check points, perform a radial sweep through the ellipse and find the upper and lower bounding angles for the angle to the check point vector.
8. Calculate the magnitude of the vector to the real time data window check point.
9. Calculate the magnitude of the collinear vector to the ellipse crossing for the real time window check point approximated by the point crossing the linear segment between the two bounding vectors as shown in Fig. 5
10. Compare the magnitude of each of the real time data check point vectors to the magnitude of each of the corresponding collinear vector ellipse crossing approximation.
11. Indicate the real time data is within the bounds of the ellipse if the magnitude of the check point vector is less than the magnitude of the corresponding collinear vector ellipse crossing approximation for all of the window check points.
12. Indicate that the real time data is overlapping the boundary of the ellipse if the magnitude of at least one check point vector is less than the magnitude of the corresponding collinear vector ellipse crossing approximation and if the magnitude of at least one check point vector is greater than the magnitude of the corresponding collinear vector ellipse crossing approximation.
13. Indicate that the real time data has exceeded the calculated yield ellipse if the magnitude of the check point vector is greater than the magnitude of the corresponding collinear vector ellipse crossing approximation for all of the window check points.
14. Repeat the process for updated real time data points.

VII. CONCLUSIONS

Transforming the resultant internal pressure and axial load or external pressure and axial load von Mises yield ellipses into a general conic equation so that a radial sweep algorithm can be used to generate the ellipses provides an efficient way of using the von Mises yield criterion for real time data test envelope verification. This process has been implemented into software that constantly monitors tests and notifies test operators when the real time data approaches or exceeds the yield ellipse.

The algorithm can be implemented in embedded software to act as an independent intelligent watchdog. It can be used for an automated corrective action request to the load control software or as an automated shutdown of the test system. Another implementation, at the expense of more calculation overhead, would be to calculate the magnitude of the verification vector \vec{v}_c using the yield ellipse itself as opposed to using a geometric approximation check. This was deemed not necessary for the intended purposes of the present implementation.

ACKNOWLEDGEMENTS

The author wishes to acknowledge the assistance, discussions and guidance from colleagues in the OCTG Test Engineering Group at Stress Engineering Services Inc.

REFERENCES

- [1] API Recommended Practice 5C5, *Procedures for Testing Casing and Tubing Connections*, American Petroleum Institute, 4th Edition, 2017, sec. 7.3
- [2] ANSI/API Technical Report 5C3, Technical Report on Equations and Calculations for Casing, Tubing, and Line Pipe Used as

Casing or Tubing; and Performance Property Tables for Casing and Tubing (ISO 10400:2007 Modified), sec. 6.4-6.6.

- [3] M. LaFuente and F. Carrois, "New drill stem rotary shoulder connection incorporates innovative single start shark thread shape," *Drilling Contractor*, March/April 2017, pp. 26-29.
- [4] J. Shigley and L. Mitchell, *Mechanical Engineering Design*, 4th ed., McGraw-Hill, 1983, 232-237.
- [5] J. F. Harvey, *Theory and Design of Pressure Vessels*, 2nd ed., 1991, pp. 56-63, pp. 276-283.
- [6] S. Timenshenko, *Strength of Materials, Part II, Advanced Theory and Problems*, D. Van Nostrand Company, 1956, pp. 205-210.
- [7] A. Bourgoine, M. Chenevert, K. Millhelm, F. Young, *Applied Drilling Engineering*, SPE Textbook Series, vol. 2, Society of Petroleum Engineers, 1986, pp. 300-311.
- [8] R. D. Cook and W. C. Young, *Advanced Mechanics of Materials*, 2nd ed., Pearson, 1985, pp. 90-96, pp. 107-110.
- [9] J. J. Tupa, *Engineering Mathematics Handbook*, 3rd ed., McGraw-Hill, 1987, pp. 44, pp. 408-409.



Donnie Curington is a senior associate at Stress Engineering Services Inc. with 26 years of engineering experience including analytical, data acquisition and control systems software development. He has developed analytical and control system software for clients and test equipment worldwide.

He has a bachelor of mechanical engineering and a master of science in mechanical engineering from Auburn University. He has taught data acquisition and software development classes for Rice University School of Continuing Studies as well as for National Instruments as a certified instructor. He was a co-founder and Manager of Engineering for Quantum Automation, was a Division Engineering Manager for Quantum Controls and was instrumental in developing a software and data acquisition training center in Houston Texas. He was a co-founder and the first chair of the inaugural Biomedical Engineering Society Industry Chapter, served as the national chair of the Biomedical Engineering Society Industry Affairs Committee and served as a board member on the Biomedical Engineering Society Board of Directors. He is the recipient of an American Society of Mechanical Engineering Meritorious Service Award.